

Strukturelle Modellierung
(Masterstudiengang Bioinformatik)

Moleküldynamiksimulation: Theorie

Sommersemester 2013

Peter Güntert

Literatur

- Andrew R. Leach: *Molecular Modelling, Principles and Applications*, Prentice Hall, 2001.
- M. P. Allen & D. J. Tildesley: *Computer Simulation of Liquids*, Clarendon Press, 1987.
- Tamar Schlick: *Molecular Modeling and Simulation*, Springer, 2006.

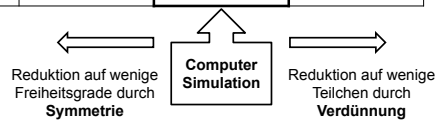
Computer-Simulation von Molekülen

Computer-Simulation von Molekülen

- Modellierung: QM, klassisch, schematisch
- Klassische Mechanik: Newton, Lagrange, Hamilton Bewegungsgleichungen
- Kartesische Koordinaten, interne Koordinaten
- Statistische Mechanik
- Simulationsmethoden: Systematische Suche, Monte Carlo, MD, Stochastische Dynamik (Langevin), Energieminimierung, Normalmodenanalyse
- Annahmen, Näherungen und Grenzen: Klassische Mechanik, Zeitskala, Systemgröße, Kraftfeld
- Geschichte der MD Simulation

Vielteilchenproblem

| | Kristalline Festkörper | Makromoleküle Flüssigkeit | Gasphase |
|---|------------------------|---------------------------------|----------|
| Quantenmechanik ($\sim N^4$) | möglich | (noch?) nicht möglich | möglich |
| Klassische Mechanik ($\sim N \log N$) | einfach | essentielle Vielteilchensysteme | trivial |



Proteinsimulation: Stufen der Vereinfachung

| Modell | Freiheitsgrade | Eliminierte Freiheitsgrade | Untersuchbare Phänomene (Beispiele) |
|---------------------------|-----------------------------------|----------------------------|-------------------------------------|
| Quantenmechanik | Kerne, Elektronen | Nukleonen | Chemische Reaktionen |
| Alle Atome, polarisierbar | Atompositionen | Elektronen | Bindung geladener Liganden |
| Alle Atome | Atompositionen (Protein + Wasser) | Polarisation | Hydratisierung |
| Alle Proteinatome | Positionen der Proteinatome | Lösungsmittel (Wasser) | Konformation in Gasphase |
| Gittermodelle | Aminosäuren | Atome | Faltung? |

Simulation von Vielteilchensystemen

System: N Atome: $i = 1, \dots, N$, Koordinaten r_i , Massen m_i , Wechselwirkung ("Kraftfeld") $V(r_1, \dots, r_N)$

Methoden:

- Systematische Suche → Ensemble
- Monte Carlo (MC) → Ensemble
- Moleküldynamik (MD) → Trajektorie
- Stochastische Dynamik (SD; Langevin) → Trajektorie
- Energieminimierung (EM) → 1 Konfiguration
- Normalmodenanalyse → 1 Konfiguration
+ harmonische Bewegung

Bewegungsgleichungen

- Newton (kartesische Koordinaten r, r):

$$m\ddot{r} = F = -\partial V(r)/\partial r$$

- Lagrange (verallgemeinerte Koordinaten q, \dot{q}):

$$d/dt (\partial L / \partial \dot{q}) - \partial L / \partial q = 0 \quad (L = T - V = E_{\text{kin}} - E_{\text{pot}})$$

- Hamilton (verallgemeinerte Koordinaten und Impulse q, p):

$$q = \partial H / \partial p, \quad p = -\partial H / \partial q \quad (H = T + V)$$

Erhaltungsgrößen

- Jeder kontinuierlichen Symmetrie eines mechanischen Systems entspricht eine Erhaltungsgröße. (Satz von Emmy Noether)

| Invarianz bezüglich | Erhaltungsgröße |
|---------------------|-----------------|
| Zeitverschiebung | Energie |
| Translation | Impuls |
| Rotation | Drehimpuls |

Vergleich Simulation - Experiment

• Atomare Eigenschaften

- Struktur: Positionen, Distanzen, H-Brücken
- Mobilität: B-Faktoren, Populationen
- Dynamik: Vibrationen, Relaxationsraten, Diffusion, Pfade

• Makroskopische Eigenschaften

- Thermodynamische Größen: Druck, Dichte, freie Energie, ...
- Viskosität, Kompressibilität, Dielektrizitätskonstante

Von mikroskopischen Details zu makroskopischen Größen: Statistische Mechanik

- Zustandssumme: $Z = \frac{1}{h^{3N} N!} \iint e^{-H(\vec{p}, \vec{q})/kT} d\vec{p} d\vec{q}$

- Hamilton-Funktion/Operator:
 $H(\mathbf{p}, \mathbf{q}) =$ kinetische Energie + potentielle Energie
(Wechselwirkung)

- Erzeugung eines Ensembles von Konfigurationen durch Computersimulation
- Mittelung über Ensemble und Zeit liefert makroskopische Größen

Statistische Mechanik

- **Grundprinzip:** Für ein thermodynamisches System im Gleichgewicht ist die Wahrscheinlichkeit, dass es einen Zustand der Energie E_i annimmt:

$$\text{Prob}(E_i) = \frac{1}{Z} e^{-E_i/kT}, \quad Z = \sum_{i=1}^N e^{-E_i/kT}$$

$k_B = 1.38065 \cdot 10^{-23}$ J/K: Boltzmann-Konstante

T : absolute Temperatur

Z : Zustandssumme

- Erwartungswert einer Observablen A : $\langle A \rangle = \frac{1}{Z} \sum_{i=1}^N A_i e^{-E_i/kT}$
- Thermodynamik: freie Energie $F = -k_B T \log Z$

Annahmen, Näherungen und Grenzen

- **Klassische Mechanik:**
 - keine tiefen Temperaturen ($T \approx 300$ K)
 - Bewegung der Wasserstoffatome
 - keine chemischen Reaktionen
- **Zeitskala von Prozessen:** (im atomaren Bereich)
 - bis ca. 1 μ s
 - aktivierte Prozesse: möglich
 - essentiell langsame Prozesse: nicht möglich (z.B. Proteinfaltung)
- **Systemgröße:**
 - $N \leq 10^6$ Teilchen
 - keine essentiell makroskopischen Vorgänge (z. B. kritische Phänomene, Phasenübergänge)
- **Kraftfeld:**
 - Ist die atomare Wechselwirkungsfunktion genügend genau zur Vorhersage der gewünschten Eigenschaft?

MD Simulation: Geschichte

| | |
|---|-----------------------|
| 1957: Harte Scheiben (2D) | - |
| 1964: Monoatomare Flüssigkeit | 10^{-11} s |
| 1971: Molekulare Flüssigkeit | 5×10^{-12} s |
| 1971: Flüssiges Salz | 10^{-11} s |
| 1975: Einfaches kleines Polymer | 10^{-11} s |
| 1977: Protein im Vakuum | 2×10^{-11} s |
| 1982: Einfache Membran | 2×10^{-10} s |
| 1983: Protein in Lösung | 2×10^{-11} s |
| 1986: DNA in Lösung | 10^{-10} s |
| 1989: Protein-DNA Komplex in Lösung | 10^{-10} s |
| 1991: Protein-Protein Komplex in Lösung | 10^{-9} s |
| 1998: 1 μ s Simulation eines Proteins in Lösung | 10^{-6} s |

MD Simulation: Personen und Programme



Martin Karplus
(CHARMM)



Peter Kollman (†)
(AMBER)



Herman Berendsen
(GROMACS)

Kraftfelder

Molekülmodell und Kraftfelder

- Kraftfelder: CHARMM, AMBER, GROMACS,...
- Energiefunktion: kovalente Bindungen, Bindungswinkel, Diederwinkel, nichtbindende Wechselwirkung (van der Waals und elektrostatisch), H-Brücken
- Bestimmung von Kraftkonstanten
- Paarliten und Cutoffs für nichtbindende Wechselwirkungen

Classical force fields: Examples

- **AMBER** (Assisted Model Building and Energy Refinement) - widely used for proteins and DNA
- **CHARMM** (Chemistry at HARvard Molecular Mechanics) - originally developed at Harvard by M. Karplus et al., widely used for both small molecules and macromolecules
- **GROMACS** - The force field optimized for the package of the same name, originally developed by H. Berendsen et al.
- **OPLS** (Optimized Potential for Liquid Simulations) developed by William L. Jorgensen at Yale University
- **ECEPP/2** - First force field for polypeptide molecules - developed by Harold Scheraga and colleagues, defined in torsion angle space

AMBER Force Field

$$E_{\text{pair}} = \sum_{\text{bonds}} K_r (r - r_{\text{eq}})^2 + \sum_{\text{angles}} K_\theta (\theta - \theta_{\text{eq}})^2 + \sum_{\text{dihedrals}} \frac{V_n}{2} [1 + \cos(n\phi - \gamma)] + \sum_{i < j} \left[\frac{A_{ij}}{R_{ij}^{12}} - \frac{B_{ij}}{R_{ij}^6} + \frac{q_i q_j}{\epsilon R_{ij}} \right]$$

Potenzial für kovalente Bindungen

$$\sum_{\text{bonds}} K_r (r - r_{\text{eq}})^2$$

- Summe über alle kovalenten Bindungen im Molekül
- Harmonisches Potential ("Bindung = Feder")
- Bindungen können nicht gebrochen werden
→ keine chemischen Reaktionen
- Parameter, von den Typen der kovalent gebundenen Atome abhängig:
 - K_r Kraftkonstante
 - r_{eq} Gleichgewichtsbindungslänge
- Rechenaufwand proportional zur Molekülgröße
- Bei Rechnung im Torsionswinkelraum nicht nötig

Potenzial für Bindungswinkel

$$\sum_{\text{angles}} K_\theta (\theta - \theta_{\text{eq}})^2$$

- Summe über alle Bindungswinkel im Molekül
- Harmonisches Potential
- Parameter, vom Typ der involvierten Atome abhängig:
 - K_θ Kraftkonstante
 - θ_{eq} Gleichgewichtsbindungswinkel
- Rechenaufwand proportional zur Molekülgröße
- Bei Rechnung im Torsionswinkelraum nicht nötig

Potenzial für Diederwinkel

$$\sum_{\text{dihedrals}} \frac{V_n}{2} [1 + \cos(n\phi - \gamma)]$$

- Summe über alle Diederwinkel im Molekül
- Periodisches Potential
- Parameter, vom Typ der involvierten Atome abhängig:
 - V_n Kraftkonstante
 - n Anzahl der Energiemaxima
 - γ Position des ersten Energiemaximums
- Rechenaufwand proportional zur Molekülgröße

Potenzial für uneigentliche ("improper") Diederwinkel

$$\sum_{\text{improvers}} \frac{V_n}{2} [1 + \cos(n\phi - \gamma)]$$

- Halten planare Gruppen in einer Ebene (Peptidgruppe, aromatische Ringe usw.)
- Für ausgewählte Quadrupel von Atomen
- Parameter, vom Typ der involvierten Atome abhängig:
 - V_n Kraftkonstante
 - n Anzahl der Energiemaxima
 - γ Position des ersten Energiemaximums
- Rechenaufwand proportional zur Molekülgröße

AMBER Atom Types

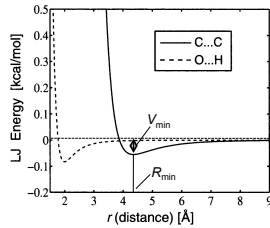
Table 1. List of Atom Types^a

| atom | type | description |
|--------|------|--|
| carbon | CT | any sp ³ carbon |
| | C | any carbonyl sp ² carbon |
| | CA | any aromatic sp ² carbon and (Cε of Arg) |
| | CM | any sp ² carbon, double bonded |
| | CC | sp ² aromatic in 5-membered ring with one substituent + next to nitrogen (Cγ in His) |
| | CV | sp ² aromatic in 5-membered ring next to carbon and lone pair nitrogen (e.g. Cδ in His (δ)) |
| | CW | sp ² aromatic in 5-membered ring next to carbon and NH (e.g. Cδ in His (ε) and in Trp) |
| | CR | sp ² aromatic in 5-membered ring next to two nitrogens (Cγ and Cε in His) |
| | CB | sp ² aromatic at junction of 5- and 6-membered rings (Cδ in Trp) and both junction atoms in Ade and Gua |
| | C* | sp ² aromatic in 5-membered ring next to two carbons (e.g. Cγ in Trp) |
| | CN | sp ² junction between 5- and 6-membered rings and bonded to CH and NH (Cε in Trp) |
| | CK | sp ² carbon in 5-membered aromatic between N and N-R (C8 in purines) |
| | CQ | sp ² carbon in 6-membered ring between lone pair nitrogens (e.g. C2 in purines) |

| | | |
|----------|----|---|
| nitrogen | N | sp ³ nitrogen in amides |
| | NA | sp ² nitrogen in aromatic rings with hydrogen attached (e.g. protonated His, Gln, Trp) |
| | NB | sp ² nitrogen in 5-membered ring with lone pair (e.g. N7 in purines) |
| | NC | sp ² nitrogen in 6-membered ring with lone pair (e.g. N3 in purines) |
| | N* | sp ² nitrogen in 5-membered ring with carbon substituent (in purine nucleosides) |
| | N2 | sp ² nitrogen of aromatic amines and guanidinium ions |
| | N3 | sp ³ nitrogen |
| | OW | sp ³ oxygen in TIPAP water |
| | OH | sp ³ oxygen in alcohols, tyrosine, and protonated carboxylic acids |
| | OS | sp ³ oxygen in ethers |
| oxygen | O | sp ² oxygen in amides |
| | O2 | sp ² oxygen in anionic acids |
| | S | sulfur in methionine and cysteine |
| | SH | sulfur in cysteine |
| | P | phosphorus in phosphates |
| | H | H attached to N |
| | HW | H in TIPAP water |
| | HO | H in alcohols and acids |
| | HS | H attached to sulfur |
| | HA | H attached to aromatic carbon |
| hydrogen | HC | H attached to aliphatic carbon with no electron-withdrawing substituents |
| | H1 | H attached to aliphatic carbon with one electron-withdrawing substituent |
| | H2 | H attached to aliphatic carbon with two electron-withdrawing substituents |
| | H3 | H attached to aliphatic carbon with three electron-withdrawing substituents |
| | HP | H attached to carbon directly bonded to formally positive atoms (e.g. C next to NH ₃ ⁺ of lysine) |
| | H4 | H attached to aromatic carbon with one electronegative neighbor (e.g. hydrogen on C3 of Trp, C6 of Thy) |
| | H5 | H attached to aromatic carbon with two electronegative neighbors (e.g. H8 of Ade and Gua and H2 of Ade) |

Lennard-Jones Potenzial

$$\sum_{i < j} \left[\frac{A_{ij}}{R_{ij}^{12}} - \frac{B_{ij}}{R_{ij}^6} \right]$$



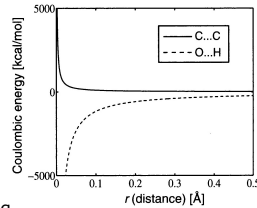
- Schwacher anziehender Beitrag: Van der Waals Kraft
- Starke Abstoßung für kurze Abstände R_{ij} aufgrund des Pauli-Prinzips
- A_{ij} = V_{ij,min} R_{ij,min}¹², B_{ij} = 2V_{ij,min} R_{ij,min}⁶ mit
 - V_{ij,min} = (V_{i,min} V_{j,min})^{1/2} Potenzialminimum
 - R_{ij,min} = R_{i,min} + R_{j,min} energetisch günstigster Abstand
- Kurzreichweitig

AMBER Atom Types

| | | | | Lennard-Jones | | | |
|-------|---------|--------|--------|---------------|---------------------|---------------------|--------|
| | | | | Mass | R _{ij,min} | V _{ij,min} | |
| TYPES | | | | | | | |
| C | 12.0100 | 1.9080 | 0.0860 | HS | 1.0080 | 0.6000 | 0.0157 |
| C* | 12.0100 | 1.9080 | 0.0860 | HW | 1.0080 | 0.0000 | 0.0000 |
| CA | 12.0100 | 1.9080 | 0.0860 | HU | 1.0080 | 0.0000 | 0.0000 |
| CB | 12.0100 | 1.9080 | 0.0860 | HV | 1.0080 | 0.0000 | 0.0000 |
| CC | 12.0100 | 1.9080 | 0.0860 | N | 14.0100 | 1.8240 | 0.1700 |
| CK | 12.0100 | 1.9080 | 0.0860 | N* | 14.0100 | 1.8240 | 0.1700 |
| CM | 12.0100 | 1.9080 | 0.0860 | N2 | 14.0100 | 1.8240 | 0.1700 |
| CN | 12.0100 | 1.9080 | 0.0860 | N3 | 14.0100 | 1.8240 | 0.1700 |
| OQ | 12.0100 | 1.9080 | 0.0860 | NA | 14.0100 | 1.8240 | 0.1700 |
| CR | 12.0100 | 1.9080 | 0.0860 | NB | 14.0100 | 1.8240 | 0.1700 |
| CT | 12.0100 | 1.9080 | 0.1094 | NC | 14.0100 | 1.8240 | 0.1700 |
| CV | 12.0100 | 1.9080 | 0.0860 | O | 16.0000 | 1.6612 | 0.2100 |
| CW | 12.0100 | 1.9080 | 0.0860 | O2 | 16.0000 | 1.6612 | 0.2100 |
| H | 1.0080 | 0.6000 | 0.0157 | OH | 16.0000 | 1.7210 | 0.2104 |
| H1 | 1.0080 | 1.3870 | 0.0157 | OS | 16.0000 | 1.6837 | 0.1700 |
| H2 | 1.0080 | 1.2870 | 0.0157 | OW | 16.0000 | 1.7683 | 0.1520 |
| H3 | 1.0080 | 1.1870 | 0.0157 | OT | 16.0000 | 1.7683 | 0.1520 |
| H4 | 1.0080 | 1.4090 | 0.0150 | OU | 16.0000 | 1.7699 | 0.1550 |
| H5 | 1.0080 | 1.3590 | 0.0150 | MU | 1.0000 | 0.0000 | 0.0000 |
| HA | 1.0080 | 1.4590 | 0.0150 | OV | 16.0000 | 1.7766 | 0.1554 |
| HC | 1.0080 | 1.4870 | 0.0157 | P | 30.9700 | 2.1000 | 0.2000 |
| HO | 1.0080 | 0.0000 | 0.0000 | S | 32.0600 | 2.0000 | 0.2500 |
| HP | 1.0080 | 1.1000 | 0.0157 | SH | 32.0600 | 2.0000 | 0.2500 |

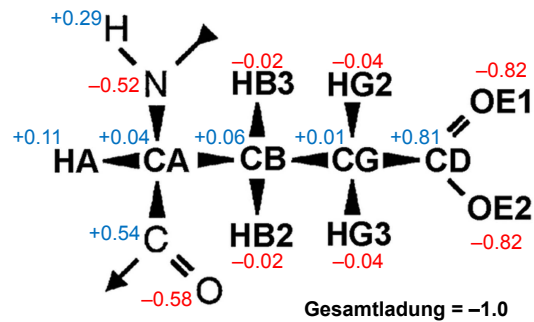
Elektrostatishes (Coulomb) Potenzial

$$\sum_{i < j} \frac{q_i q_j}{\epsilon R_{ij}}$$



- Partialladungen q_i, q_j
- Dielektrizitätskonstante ε beschreibt (gemittelte) Polarisierbarkeit der Umgebung
 - ε_{Wasser} ≈ 80; ε_{apolar} ≈ 2.
 - Werden alle Ladungen explizit behandelt: ε = 1
- Langreichweitig!
- Stark!
- Wichtigster Energiebeitrag auch für Wasserstoffbrücken

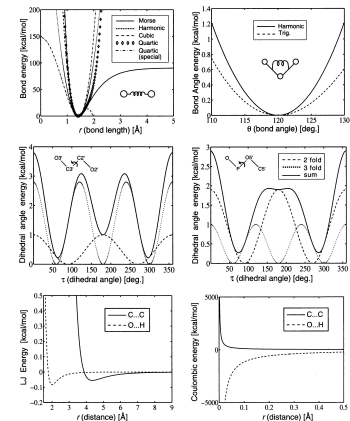
Partiellladungen (Glu, AMBER)



Bestimmung von Kraftfeldparametern

- **Fit der Energie zu quantenmechanischen *ab initio* Rechnungen**
 - z.B. Partialladungen
- **Fit zu experimentellen Daten**
 - Infrarot-Spektroskopie (Vibrationen)
 - Röntgenkristallographie (Geometrie)
 - NMR Spektroskopie
 - Thermodynamische Eigenschaften
- **Schwierigkeiten**
 - Exakte Beziehung molekulare Eigenschaft ↔ Kraftfeldparameter
 - Konzeptionelle Einfachheit ↔ Anzahl Parameter
 - Gegenseitige Abhängigkeit von Kraftfeldparametern
 - Widersprüchliche Anforderungen für Verbesserungen der Parameter
 - Einfluss von Näherungen
- **Genauigkeit wird durch den ungenaueren Term der Energiefunktion bestimmt.**

Energierme



Strukturelle Modellierung
(Masterstudiengang Bioinformatik)

Moleküldynamiksimulation: Theorie

Sommersemester 2013

Peter Güntert

Literatur

- Andrew R. Leach: *Molecular Modelling, Principles and Applications*, Prentice Hall, 2001.
- M. P. Allen & D. J. Tildesley: *Computer Simulation of Liquids*, Clarendon Press, 1987.
- Tamar Schlick: *Molecular Modeling and Simulation*, Springer, 2006.

Kraftberechnung

- Kraft = $-\text{Gradient}$ der potentiellen Energie
- Analytisch berechnete partielle Ableitungen der potentiellen Energie nach den Koordinaten aller Atome sind notwendig für klassische MD Simulation.
- MD im Torsionswinkelraum benötigt partielle Ableitungen der potentiellen Energie nach den Torsionswinkeln.

Paarlisten

- N Atome \rightarrow ca. $N(N-1)/2$ Paarwechselwirkungen
- Berechnung der nichtbindenden Wechselwirkung ist aufwendigster Teil der Kraftberechnung
- Potenzial nimmt mit der Entfernung ab \rightarrow Vernachlässigung von kleinen Termen = langen Distanzen
- Kurze Distanzen $R < R_{\max}$ werden periodisch in Paarliste gespeichert
- Wechselwirkungen werden nur für Atompaare mit Abstand $R < R_{\text{cutoff}} < R_{\max}$ berechnet
- Langreichweitige elektrostatische WW $\rightarrow R_{\text{cutoff}} \approx 12 \text{ \AA}$
- Aktualisierung der Paarliste nach einer festen Anzahl Zeitschritten oder wenn sich ein Teilchen $R_{\max} - R_{\text{cutoff}}$ weit bewegt hat.

Paarliste und Cutoff

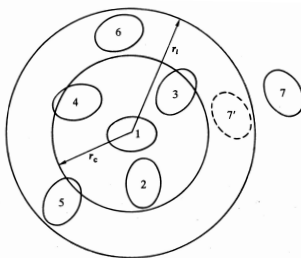
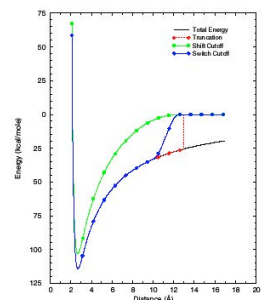


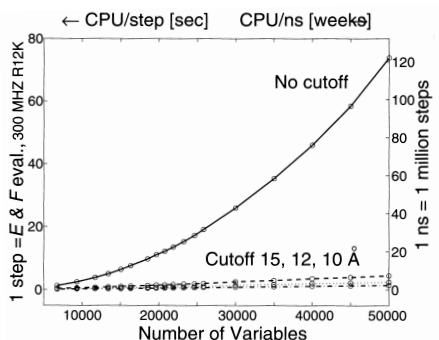
Fig. 5.4 The cutoff sphere, and its skin, around a molecule 1. Molecules 2, 3, 4, 5, and 6 are on the list of molecule 1; molecule 7 is not. Only molecules 2, 3, and 4 are within the range of the potential at the time the list is constructed.

Treatment of truncation effects

- **Truncation:** the interactions are simply set to zero for interatomic distances greater than the cutoff distance. This method can lead to large fluctuations in the energy. This method is not often used.
- **SHIFT cutoff method:** this method modifies the entire potential energy surface such that at the cutoff distance the interaction potential is zero. The drawback of this method is that equilibrium distances are slightly decreased.
- **SWITCH cutoff method:** This method tapers the interaction potential over a predefined range of distances. The potential takes its usual value up to the first cutoff and is then switched to zero between the first and last cutoff. This model suffers from strong forces in the switching region which can slightly perturb the equilibrium structure. The SWITCH function is not recommended when using short cutoff regions.



Rechenzeit mit und ohne Cutoff



MD Algorithmen

MD Algorithmen

- Energieminimierung
- Integration der Bewegungsgleichungen
- Temperaturkontrolle
- Druckkontrolle
- Periodische Randbedingungen

Energieflächen

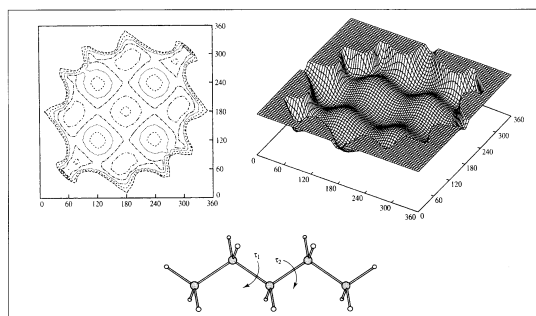


Fig. 5.1. Variation in the energy of pentane with the two torsion angles indicated and represented as a contour diagram and isometric plot. Only the lowest-energy regions are shown.

Lokale Minima, globales Minimum

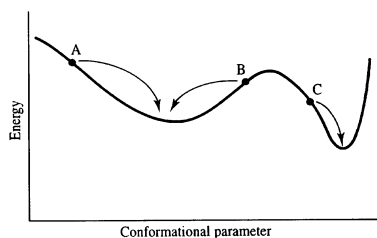


Fig. 5.3: A schematic one-dimensional energy surface. Minimisation methods move downhill to the nearest minimum. The statistical weight of the narrow, deep minimum may be less than a broad minimum which is higher in energy.

Energieminimierungsalgorithmen

- Ohne Ableitungen
- Mit Gradienten:
 - Steilster Abstieg (steepest descent)
 - konjugierte Gradienten (conjugate gradients)
- Mit zweiter Ableitung: Newton-Raphson Methode

Simplex Algorithmus

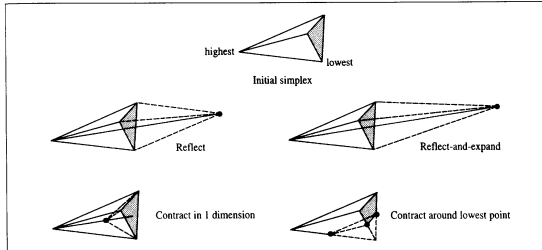


Fig. 5.4: The three basic moves permitted to the simplex algorithm (reflection, and its close relation reflect-and-expand; contract in one dimension and contract around the lowest point). (Figure adapted from Press WH, B P Flannery, S A Teukolsky and WT Vetterling 1992. Numerical Recipes in Fortran. Cambridge, Cambridge University Press.)

Simplex Algorithmus

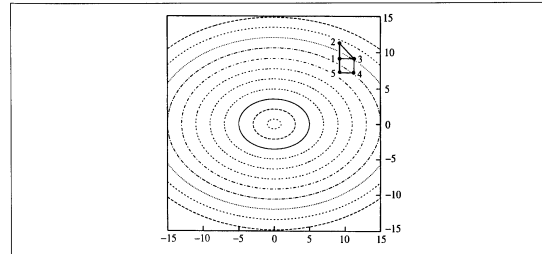


Fig. 5.5: The first few steps of the simplex algorithm with the function $x^2 + 2y^2$. The initial simplex corresponds to the triangle 123. Point 2 has the largest value of the function and the next simplex is the triangle 134. The simplex for the third step is 145.

Eindimensionale Minimierung

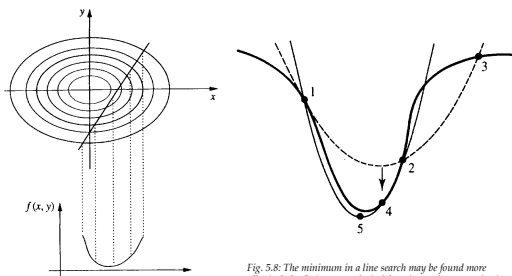


Fig. 5.7: A line search is used to locate the minimum in the function in the direction of the gradient.

Fig. 5.8: The minimum in a line search may be found more effectively by fitting an analytical function such as a quadratic to the initial set of three points (1,2 and 3). A better estimate of the minimum can then be found by fitting a new function to the points 1, 2 and 4 and finding its minimum.

Energieminimierung: Steepest descent

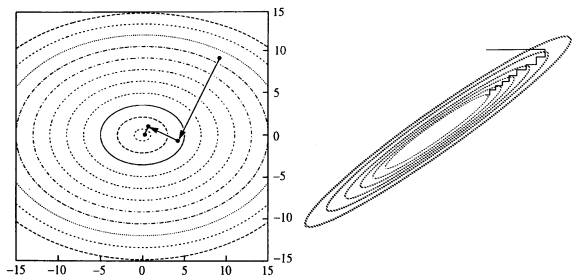


Fig. 5.9: Application of steepest descents to the function $x^2 + 2y^2$.

Fig. 5.10: The steepest descents method can give undesirable behaviour in a long narrow valley.

Konjugierte Gradientenmethode

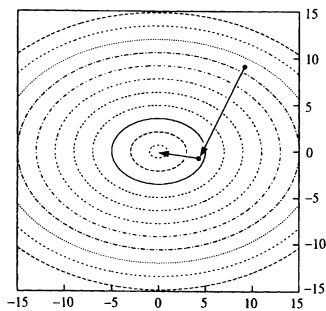


Fig. 5.11: Application of conjugate gradients method to the function $x^2 + 2y^2$.

Taylor Reihenentwicklung

$$f(x) = f(x_0) + f'(x_0)(x - x_0) + \frac{f''(x_0)}{2}(x - x_0)^2 + \frac{f'''(x_0)}{3!}(x - x_0)^3 + \dots$$

$$\mathbf{r}(t + \delta t) = \mathbf{r}(t) + \delta t \mathbf{v}(t) + \frac{1}{2} \delta t^2 \mathbf{a}(t) + \frac{1}{6} \delta t^3 \mathbf{b}(t) + \frac{1}{24} \delta t^4 \mathbf{c}(t) + \dots$$

$$\mathbf{v}(t + \delta t) = \mathbf{v}(t) + \delta t \mathbf{a}(t) + \frac{1}{2} \delta t^2 \mathbf{b}(t) + \frac{1}{6} \delta t^3 \mathbf{c}(t) + \dots$$

$$\mathbf{a}(t + \delta t) = \mathbf{a}(t) + \delta t \mathbf{b}(t) + \frac{1}{2} \delta t^2 \mathbf{c}(t) + \dots$$

$$\mathbf{b}(t + \delta t) = \mathbf{b}(t) + \delta t \mathbf{c}(t) + \dots$$

Verlet Algorithmus

The Verlet algorithm uses the positions and accelerations at time t , and the positions from the previous step, $\mathbf{r}(t - \delta t)$, to calculate the new positions at $t + \delta t$, $\mathbf{r}(t + \delta t)$. We can write down the following relationships between these quantities and the velocities at time t :

$$\mathbf{r}(t + \delta t) = \mathbf{r}(t) + \delta t \mathbf{v}(t) + \frac{1}{2} \delta t^2 \mathbf{a}(t) + \dots \quad (7.6)$$

$$\mathbf{r}(t - \delta t) = \mathbf{r}(t) - \delta t \mathbf{v}(t) + \frac{1}{2} \delta t^2 \mathbf{a}(t) - \dots \quad (7.7)$$

Adding these two equations gives

$$\mathbf{r}(t + \delta t) = 2\mathbf{r}(t) - \mathbf{r}(t - \delta t) + \delta t^2 \mathbf{a}(t) \quad (7.8)$$

The velocities do not explicitly appear in the Verlet integration algorithm. The velocities can be calculated in a variety of ways; a simple approach is to divide the difference in positions at times $t + \delta t$ and $t - \delta t$ by $2\delta t$:

$$\mathbf{v}(t) = [\mathbf{r}(t + \delta t) - \mathbf{r}(t - \delta t)] / 2\delta t \quad (7.9)$$

Alternatively, the velocities can be estimated at the half-step, $t + \frac{1}{2} \delta t$:

$$\mathbf{v}(t + \frac{1}{2} \delta t) = [\mathbf{r}(t + \delta t) - \mathbf{r}(t)] / \delta t \quad (7.10)$$

Leap-frog Algorithmus

The *leap-frog* algorithm uses the following relationships:

$$\mathbf{r}(t + \delta t) = \mathbf{r}(t) + \delta t \mathbf{v}(t + \frac{1}{2} \delta t) \quad (7.11)$$

$$\mathbf{v}(t + \frac{1}{2} \delta t) = \mathbf{v}(t - \frac{1}{2} \delta t) + \delta t \mathbf{a}(t) \quad (7.12)$$

To implement the leap-frog algorithm, the velocities $\mathbf{v}(t + \frac{1}{2} \delta t)$ are first calculated from the velocities at time $t - \frac{1}{2} \delta t$ and the accelerations at time t . The positions $\mathbf{r}(t + \delta t)$ are then deduced from the velocities just calculated together with the positions at time $\mathbf{r}(t)$ using Equation (7.11). The velocities at time t can be calculated from

$$\mathbf{v}(t) = \frac{1}{2} [\mathbf{v}(t + \frac{1}{2} \delta t) + \mathbf{v}(t - \frac{1}{2} \delta t)] \quad (7.13)$$

The velocities thus 'leap-frog' over the positions to give their values at $t + \frac{1}{2} \delta t$ (hence the name). The positions then leap over the velocities to give their new values at $t + \delta t$, ready for the velocities at $t + \frac{3}{2} \delta t$, and so on. The leap-frog method has two advantages over the

Velocity Verlet Algorithmus

The *velocity Verlet* method [Swope *et al.* 1982] gives positions, velocities and accelerations at the same time and does not compromise precision:

$$\mathbf{r}(t + \delta t) = \mathbf{r}(t) + \delta t \mathbf{v}(t) + \frac{1}{2} \delta t^2 \mathbf{a}(t) \quad (7.14)$$

$$\mathbf{v}(t + \delta t) = \mathbf{v}(t) + \frac{1}{2} \delta t [\mathbf{a}(t) + \mathbf{a}(t + \delta t)] \quad (7.15)$$

The velocity Verlet method is actually implemented as a three-stage procedure because, as can be seen from Equation (7.15), to calculate the new velocities requires the accelerations at both t and $t + \delta t$. Thus in the first step the positions at $t + \delta t$ are calculated according to Equation (7.14) using the velocities and the accelerations at time t . The velocities at time $t + \frac{1}{2} \delta t$ are then determined using:

$$\mathbf{v}(t + \frac{1}{2} \delta t) = \mathbf{v}(t) + \frac{1}{2} \delta t \mathbf{a}(t) \quad (7.16)$$

New forces are next computed from the current positions, thus giving $\mathbf{a}(t + \delta t)$. In the final step, the velocities at time $t + \delta t$ are determined using:

$$\mathbf{v}(t + \delta t) = \mathbf{v}(t + \frac{1}{2} \delta t) + \frac{1}{2} \delta t \mathbf{a}(t + \delta t) \quad (7.17)$$

Beemans Algorithmus

Beeman's algorithm [Beeman 1976] is also related to the Verlet method:

$$\mathbf{r}(t + \delta t) = \mathbf{r}(t) + \delta t \mathbf{v}(t) + \frac{3}{8} \delta t^2 \mathbf{a}(t) - \frac{1}{8} \delta t^2 \mathbf{a}(t - \delta t) \quad (7.18)$$

$$\mathbf{v}(t + \delta t) = \mathbf{v}(t) + \frac{3}{8} \delta t \mathbf{a}(t) + \frac{5}{8} \delta t \mathbf{a}(t) - \frac{1}{8} \delta t \mathbf{a}(t - \delta t) \quad (7.19)$$

The Beeman integration scheme uses a more accurate expression for the velocity. As a consequence it often gives better energy conservation, because the kinetic energy is calculated directly from the velocities. However, the expressions used are more complex than those of the Verlet algorithm and so it is computationally more expensive.

Gear Predictor-Corrector Algorithms

The predictor-corrector methods [Gear 1971] form a general family of integration algorithms from which one can select a scheme that is correct to a given order. These methods have three basic steps. First, new positions, velocities, accelerations and higher-order terms are predicted according to the Taylor expansion, Equations (7.2)-(7.4). In the second stage, the forces are evaluated at the new positions to give accelerations $\mathbf{a}(t + \delta t)$. These accelerations are then compared with the accelerations that are predicted from the Taylor series expansion, $\mathbf{a}^c(t + \delta t)$. The difference between the predicted and calculated accelerations is then used to 'correct' the positions, velocities, etc., in the correction step:

$$\Delta \mathbf{a}(t + \delta t) = \mathbf{a}^c(t + \delta t) - \mathbf{a}(t + \delta t) \quad (7.22)$$

Then

$$\mathbf{r}^f(t + \delta t) = \mathbf{r}(t + \delta t) + c_0 \Delta \mathbf{a}(t + \delta t) \quad (7.23)$$

$$\mathbf{v}^f(t + \delta t) = \mathbf{v}(t + \delta t) + c_1 \Delta \mathbf{a}(t + \delta t) \quad (7.24)$$

$$\mathbf{a}^c(t + \delta t) / 2 = \mathbf{a}(t + \delta t) / 2 + c_2 \Delta \mathbf{a}(t + \delta t) \quad (7.25)$$

$$\mathbf{b}^f(t + \delta t) / 6 = \mathbf{b}(t + \delta t) / 6 + c_3 \Delta \mathbf{a}(t + \delta t) \quad (7.26)$$

Gear has suggested 'best' values of the coefficients c_0, c_1, \dots . The set of coefficients to use depends upon the order of the Taylor series expansion. In Equations (7.23)-(7.26) the expansion has been truncated after the third derivative of the positions (i.e. $\mathbf{b}(t)$). The appropriate set of coefficients to use in this case is $c_0 = \frac{1}{2}$, $c_1 = \frac{5}{6}$, $c_2 = 1$ and $c_3 = \frac{1}{3}$.

Energiefluktuation

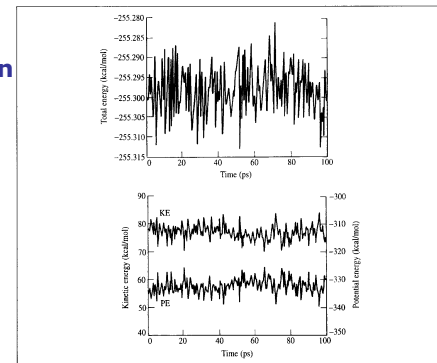


Fig. 7.3: Variation in total energy versus time for the production phase of a molecular dynamics simulation of 256 argon atoms at a temperature of 100 K and a density of 1.396 g cm^{-3} (top). The time step was 10 fs and the equations of motion were integrated using the velocity Verlet algorithm. The variations in the kinetic and potential energies are also shown (bottom). The graphs have different scales.

Zeitschrittlänge

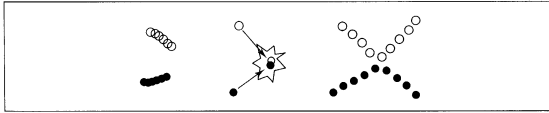


Fig. 7.4: With a very small time step (left) phase space is covered very slowly; a large time step (middle) gives instabilities. With an appropriate time step (right) phase space is covered efficiently and collisions occur smoothly.

| System | Types of motion present | Suggested time step (s) |
|------------------------------------|---|-----------------------------------|
| Atoms | Translation | 10^{-14} |
| Rigid molecules | Translation and rotation | 5×10^{-15} |
| Flexible molecules, rigid bonds | Translation, rotation, torsion | 2×10^{-15} |
| Flexible molecules, flexible bonds | Translation, rotation, torsion, vibration | 10^{-15} or 5×10^{-16} |

Table 7.1 The different types of motion present in various systems together with suggested time steps.

Energieerhaltung

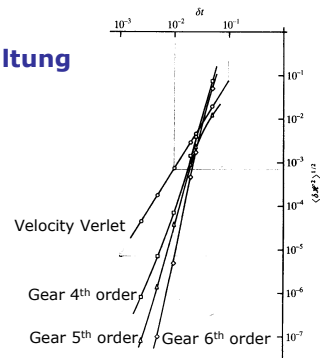


Fig. 3.3 Energy conservation of various algorithms. The system studied is as for Fig. 3.1. We calculate RMS energy fluctuations $\langle \delta E^2 \rangle^{1/2}$ for various runs starting from the same initial conditions, and proceeding for the same total simulation time t_{sim} but using different time steps Δt and corresponding numbers of steps $n_{sim} = t_{sim}/\Delta t$. The plot uses log-log scales. The curves correspond to velocity Verlet (circles), Gear fourth-order (squares), Gear fifth-order (triangles), and Gear sixth-order (diamonds) algorithms.

Temperatur

Momentane Temperatur $T(t)$:

$$\frac{1}{2} N k_B T(t) = E_{kin}(t) = \sum_{i=1}^n \frac{1}{2} m_i v_i^2$$

N = Anzahl Freiheitsgrade ($N = 3n$), n = Anzahl Atome

Methoden für MD Simulation bei konstanter Temperatur:

- (strikt) konstante kinetische Energie und Temperatur
- erweitertes System mit zusätzlichem Freiheitsgrad
- schwache Kopplung an ein Wärmebad

Druck

Druck = Kraft pro Flächeneinheit auf die Wände des Systems
Aber: bei periodischen Randbedingungen keine Wand vorhanden

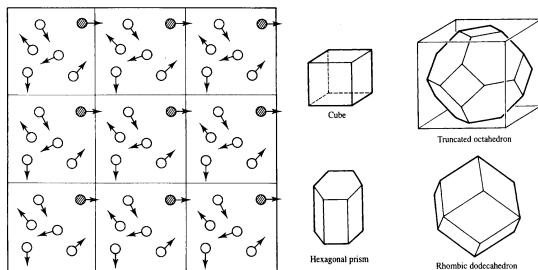
$$\text{Virialsatz: } P = \frac{2}{3V} \left[E_{kin} + \frac{1}{2} \sum_{i=1}^n \vec{r}_{ij} \cdot \vec{F}_{ij} \right]$$

P = Druck, V = Volumen

Methoden für MD Simulation bei konstantem Druck:

- (strikt) konstanter Druck
- erweitertes System mit zusätzlichem Freiheitsgrad
- schwache Kopplung

Periodische Randbedingungen



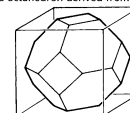
Periodische Randbedingungen

Rectangular box, side $2a$ (x) by $2b$ (y) by $2c$ (z)



```
x = x - 2 * a * AINT(x/a)
y = y - 2 * b * AINT(y/b)
z = z - 2 * c * AINT(z/c)
A common alternative is:
x = x - a * AINT(x/a)
y = y - b * AINT(y/b)
z = z - c * AINT(z/c)
```

Truncated octahedron derived from cube of side $2a$



```
x = x - 2 * a * AINT(x/a)
y = y - 2 * b * AINT(y/a)
z = z - 2 * c * AINT(z/a)
if (ABS(x) + ABS(y) + ABS(z)) >= 1.5 * A
then
  x = x - SIGN(a, x)
  y = y - SIGN(a, y)
  z = z - SIGN(a, z)
endif
```

Hexagonal prism of length $2a$ (in z direction) and distance between opposite faces of the hexagon $2b$



```
z = z - 2 * a * AINT(z/a)
x = x - 2 * b * AINT(x/b)
if (ABS(x) + sqrt(3) * ABS(y)) >= 2 * b then
  x = x - SIGN(b, x)
  y = y - SIGN(sqrt(3) * b, y)
endif
```